# CORRELATION BETWEEN MIXING HEIGHT AND CONCENTRATIONS OF AIR POLLUTANTS IN THE TAIPEI BASIN

**Charles C. K. Chou[(1)], C. T. Lee[(2)], W. N. Chen[(1)], S. Y. Chang[(1)], T. K. Chen[(1)], C. Y. Lin[(1)], J. P. Chen[(3)]**

*[(1)]Research Center for Environmental Changes, Academia Sinica, Taipei 115, Taiwan, R.O.C.*
*E-mail: ckchou@rcec.sinica.edu.tw*
*[(2)]Graduate Institute of Environmental Engineering, National Central University, ChungLi 320, Taiwan, R.O.C.*
*E-mail: ctlee@cc.ncu.edu.tw*
*[(3)]Department of Atmospheric Sciences, National Taiwan University, Taipei 106, Taiwan, R.O.C.*
*E-mail: jpchen@webmail.as.ntu.edu.tw*

## ABSTRACT

A LIDAR system was used to measure the depth of the atmospheric mixing layer over Taipei, Taiwan in the spring of 2005. This paper presents the variations of the mixing height and the mixing ratios of air pollutants during an episode of air quality deterioration (March 7-10), when Taipei was under an anti-cyclonic outflow of a traveling high- pressure system. The consistency between the changes in the mixing height and in the ambient temperature implied that the mixing layer dynamics were dominated by solar thermal forcing. In addition, the synoptic condition is dominated by a high-pressure system within which advection and convection were inhibited, causing the mixing layer to be shallow in the afternoon. As the cap of the mixing layer descended substantially in the afternoon, reduced dispersion caused the concentrations of primary air pollutants to increase sharply. Consequently, the pollutant concentration exhibited an anti-correlation with the mixing height. The results indicate the critical role of the mixing layer dynamics in the formation of a pollution episode, and demonstrate the application value of the LIDAR technique.

## 1. INTRODUCTION

The mixing layer is the lowest part of the atmosphere where the constituents of air are mixed due to convection and mechanical turbulence over the ground. The dispersion of air pollutants is often confined within the mixing layer, the depth of the mixing layer, which is usually referred to as the "mixing height", is one of the most critical parameters in air quality studies. For decades, there has been a consensus that the deterioration of air quality is usually caused by the formation of a shallow mixing layer. However, to date, mixing height is not measured routinely at most air quality stations. In recent years, continuous measurements of the mixing height have been successfully carried out using the aerosol LIDAR technique [1][2][3]. With the advantages of a high temporal resolution, LIDAR can provide valuable data for understanding the mixing layer dynamics. Furthermore, as the aerosol itself is one of the major air pollutants in an urban atmosphere, the LIDAR signals are essential for understanding the vertical distribution of air pollutants.

Analyses of the seasonal variations of the air pollutants in Taipei, Taiwan show that their concentrations usually reached the maxima in spring. In addition to possible long-range transport from Asian pollution outbreaks [4], local factors such as a shallow mixing layer may also contribute to the high pollution in springtime. In this study, a LIDAR system was used to measure the mixing height over Taipei, Taiwan during a spring pollution episode. The drastic variations of the mixing height and its implications for the high levels of air pollutants are discussed. Meteorological conditions and mechanism for the development of a shallow mixing layer in the afternoon are identified. The results indicate the critical role of the mixing layer dynamics in the formation of a pollution episode, and demonstrate the application value of the LIDAR technique.

## 2. DATA SOURCES AND INSTRUMENTATION

### 2.1 Data sources

Data used in this study include the mass concentrations of PM10 and PM2.5 and light scattering coefficient (at 550 nm) measured at the Taipei (SinJhuang) Supersite, and gaseous air pollutants (CO, $O_3$, $SO_2$, $NO_x$, THC/NMHC) measured at the SinJhuang air quality monitoring station of Taiwan EPA, as well as meteorological parameters (barometric pressure, ambient temperature, and surface wind field) measured at the BanChio observatory of the Central Weather Bureau of Taiwan. In addition, vertical profiles of aerosol in the troposphere, and the depth of the mixing layer over Taipei were obtained from a ground-based LIDAR system installed on campus of the National Taiwan University. All measurements were assimilated with a

time resolution of 1 hour. These measurement sites are within 10 kilometers of each other.

### 2.2 LIDAR data processing and mixing height determination

The signal detected by LIDAR is usually described in terms of the range-squared-corrected signal (RSCS). The aerosol concentration in the mixing layer is significantly higher than in the free troposphere, the cap of the mixing layer is characterized by a deep gradient of the aerosol backscattering signal. Flamant et al. [2] proposed that the altitude of the top of the mixing layer could be obtained from the profile of the derivative of the LIDAR signal (i.e. RSCS). Accordingly, in this study, the mixing height is defined at the altitude with the minimum of the first derivative of RSCS (i.e. $dPz^2/dz$).

## 3. RESULTS AND DISCUSSION

### 3.1 Meteorological conditions

A strong traveling high-pressure system moved along the $30^oN$ latitude line, from the Southeast China into the West Pacific Ocean during the period of March 6-10, 2005. Fig. 1(a) illustrates that the barometric pressure (BP) at Taipei reached a high level of 1030 hPa in the early morning of March 6, indicating that Taipei was rather close to the high center. As the high-pressure system was moving away, leaving Taipei under its anti-cyclonic subsidence, the BP gradually decreased and during that time the ambient temperature (AT) varied with typical diurnal cycles until the next cold front arrived in the early morning of March 11. The variations of the surface winds are shown in Fig. 1(b). It were characterized by weak synoptic winds during March 7-10. Under this setting, moderate sea breezes (2-3 m/s) developed each afternoon as a result of the land-heating effects. It is worth noting that the wind speed decreased drastically while the ambient temperature declined, and that the sea-breeze peaks in Fig. 1(b) are exactly coincidental with those of the ambient temperature shown in Fig. 1(a). The synchronization between the ambient temperature and the wind speed implies that thermo-forcing was dominant in the boundary layer dynamics in those days, when Taipei was on the leeward side of the high mountains located on the southeastern rim of the basin.

### 3.2 Variations in mixing height

Fig. 2(a)-(b) show the time-altitude evolution of the aerosol backscattering coefficient and the first derivative of the LIDAR signal, respectively, for March 7, 2005. In the morning, most of the aerosols were confined below the surface inversion that positioned at 500-800 m above the ground level (AGL). However, at around 1 km AGL there is another layer of relatively high aerosol concentrations. This aerosol layer is most likely remnants of the convectively elevated mixing layer from the previous day. The surface inversion started to break up at about 08:00 LST and the mixing layer was thickening. The LIDAR signals clearly show the evolution of the atmospheric boundary layer, transforming from a stratified to a well-mixed structure in the morning. The mixing height reached a maximum of 1460 m AGL at noon. Fig. 2(c) illustrates the well mixed structure at this time with the vertical profile of the backscattering coefficient. In the afternoon toward the evening, the mixing height gradually lowered while a residual layer remained between the caps of the mixing layer and the boundary layer as the stable nocturnal surface layer was forming again. The evolution of the boundary layer observed in our study agrees with those documented in the literature [2][5]. This consistency warrants a further analysis of the boundary layer dynamics based on the LIDAR measurements.

It is worth noting that the mixing height decreased drastically in the afternoon, implying that the development of the nocturnal boundary layer could have started several hours prior to sunset. Consequently, a substantial amount of air pollutants could have been stored in the residual layer and negatively influencing the air quality in the downwind area as the mixing layer developed in the next morning. Such a drastic decrease of the mixing height in the afternoon is similar to that observed by Strawbridge and Snyder [3] in British Columbia, Canada. However, it's unusual for it to occur in subtropical areas like Taiwan. Therefore the cause of this phenomenon is of great interest and importance.

Fig. 3(a) shows the variation of mixing height during the period of this study. Changes in mixing height during daytime (10:00-18:00 LST) are coherent with the changes in ambient temperature, as shown by the good statistical correlation in Fig. 3(b). The hourly increase in mixing height was linearly proportional to the increase in ambient temperature of the previous hour, which means a lag of about 1 hour from the heating up of the air mass to the growth of the mixing layer. Considering the correlations shown in Fig. 3(b) and the meteorological conditions described in the previous section, we can draw the conclusion that the drastic decrease in mixing height was a result of the sharp temperature drop in the afternoon. When the thermal forcing ceased, the convective mixing had to rely on the dynamics of the weather systems. However, as the traveling high-pressure system was just located nearby, Taipei was in the subsidence zone and the convective mixing was suppressed. For instance, on March 7 the drop of air temperature from 12:00 to 18:00 was -8.1°C. According to the regression trend shown in Fig. 3b, the

mixing height would have decreased from 1460 to 115 m, which is below the detection range of our LIDAR system.

### 3.3 Variations of air quality

During the period of March 7-10, 2005, Taipei experienced an episode of serious air quality deterioration exactly when a slow-moving high-pressure system was nearby. Fig. 4 shows the hourly PM10 (divided into PM2.5 and PM2.5-10 counterparts) concentrations measured at the Taipei supersite during this episode. Although the LIDAR was turned off for maintenance during the daytime hours of March 8, it is reasonable to expect that a mixing layer should had developed as was the case on March 7 given the similar diurnal patterns of AT and the surface winds shown in Fig. 1. With the measured hourly AT (see Fig. 1) and assuming a mixing height of 0.3 km for 08:00 LST, the daytime mixing height on March 8 can be estimated by applying the regression model shown in Fig. 3(b). The estimated maximal mixing height is 1.8 km occurring at 14:00 LST. The convective mixing led to the decrease in concentration of the air pollutants around noon. Substantial increases of the pollutant concentrations were also observed in the afternoon of March 8. In fact, a drastic rise in the pollutant concentrations occurred in the afternoon of each day during this episode. In addition to the particulate matters, almost all the air pollutants exhibited similar diurnal patterns during this period. The patterns of the gaseous species are even more self-consistent and clearer than those of the aerosols, indicating that the mixing efficiency for gaseous species is better than for aerosols, particularly the coarse particles.

Table 1 summarizes the linear correlation coefficients between the mixing height and the ambient concentration of each air pollutant for the time periods of 13:00-18:00 of March 7 and March 9-10, respectively. On March 7, prior to the episode, the correlation was relatively weak. In contrast, on March 10, almost perfect anti-correlations exist between the mixing height and the pollutant concentrations were found. The concentrations of air pollutants and the light scattering by aerosols increased proportionally when the mixing height decreased in the afternoon. This showed that the air pollutants were concentrated when the cap of the mixing layer was descending. It is worth noting that the ozone concentration was positively correlated with the mixing height. The diurnal cycle of ozone mixing ratio indicates that photochemical reactions prevailed during daytime of the episode. Thus, it is reasonable to infer that substantial secondary pollutants were formed through photochemical reactions within the mixing layer. The formation of secondary aerosols may explain why the particulate matters (PM10, PM2.5, and light scattering coefficient) did not significantly decrease as did the gaseous species around noon time due to convective dispersion (figure not shown).

Another feature that is worth noting is the built up of nighttime pollutant concentrations. One factor that contributes to the daily build up of pollutants in the night is the weakening winds (shown in Fig. 1(b)). Evidently wind advection played a predominant role in the night time air quality, whereas the convective mixing predominated in the daytime. In the case where the synoptic weather conditions tended to inhibit advection, a stagnant atmosphere was formed, resulting in the accumulation of air pollutants during the night.

## 4. CONCLUSIONS

The variation of urban mixing layer and its implication for the air quality deterioration episode in Taipei, Taiwan was studied with air quality monitoring data and LIDAR measurements. We found that the urban mixing heights grow proportional to the changes in ambient air temperature with a lag of 1 hour. The cap of the mixing layer descended drastically as the thermal forcing declined in the afternoon during this springtime episode. In addition, the shallow mixing layer in the afternoon was attributed to the anti-cyclonic subsidence of a traveling high-pressure system which was passing through the north of Taiwan. Synoptic conditions inhibited advection and convection of the boundary layer air mass, and therefore reduced the mechanical forcing for the mixing layer.

During the episode examined in this study, the ambient levels of the air pollutants, except ozone, were anti-correlated consistently with the mixing height in the afternoon, indicating that the high mixing ratios of the air pollutants in the evening were resulted from a reduced dispersion volume. The mixing ratio of ozone, a typical secondary pollutant due to the photochemistry in the troposphere, exhibited a positive correlation with the mixing height. The positive correlation was a result of their common forcing, i.e. solar irradiation. Inferred from this is a substantial production of secondary aerosols, which later on accumulated and resulting in high concentrations of particulate matters in the evening.

Considering the fact that an improvement in the understanding of boundary layer dynamics will most certainly contribute to the development of an air quality forecast model, a well-designed long-term study combining LIDAR and atmospheric chemistry measurements is urgently needed.

## REFERENCES

1. Flamant, C., Pelon, J., Flamant, P.H., Durand, P., Lidar determination of the entrainment zone thickness

at the top of the unstable marine atmospheric boundary-layer, *Boundary-Layer Meteorology*, Vol. 83, 247-284, 1997.
2. Cohn, S.A. and Angevine, W.M., Boundary layer height and entrainment zone thickness measured by lidars and wind profiling radars, *Journal of Applied Meterology*, Vol. 39, 1233-1247, 2000.
3. Strawbridge, K.B., Snyder, B.J., Planetary boundary layer height determination during Pacific 2001 using the advantage of a scanning lidar instrument, *Atmos. Environ.*, Vol. 38, 5861-5871, 2004.
4. Chou, C. C.-K., Huang, S.-H., Chen, T.-K., Lin, C.-Y., Wang, L.-C., Size-segregated characterization of atmospheric aerosols in Taipei during Asian outflow episodes, *Atmospheric Research*, Vol. 75, 89-109, 2005.
5. Stull, R.B., *An introduction to boundary layer meterology*, Kluwer Academic Publishers, Netherlands, 1988.

## FIGURES AND TABLES

Table 1. The correlation coefficients between the mixing height and the ambient concentrations of the respective air pollutants in the afternoon of each day.

| | March 7 | March 9 | March 10 |
|---|---|---|---|
| PM10 | -0.0048 | -0.7460 | -0.9690 |
| PM2.5 | -0.2105 | -0.7240 | -0.9901 |
| $b_{scat}$_550nm | 0.1831 | -0.7368 | -0.9643 |
| CO | -0.7045 | -0.9268 | -0.8200 |
| $NO_x$ | -0.6280 | -0.8407 | -0.9429 |
| NMHC | -0.7111 | -0.8724 | -0.9225 |
| THC | -0.8095 | -0.8286 | -0.9440 |
| $O_3$ | 0.6929 | 0.5052 | 0.9588 |
| $SO_2$ | 0.4139 | -0.8432 | 0.0088 |

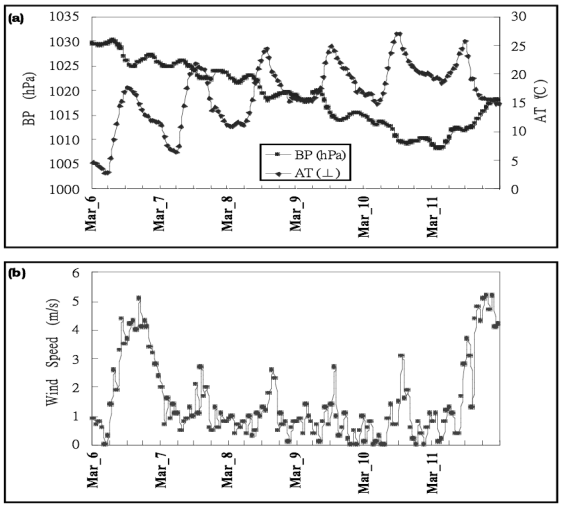


Fig. 1. Hourly variations of (a) barometric pressure and ambient temperature; (b) surface wind speed during the episode of this study.

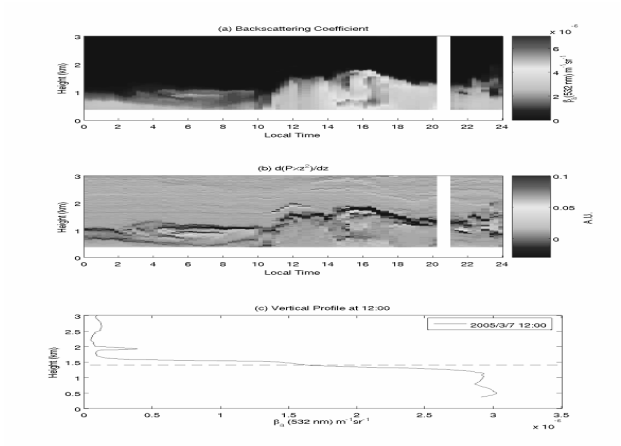


Fig. 2. Evolution of LIDAR measurements on March 7, 2005. (a) backscattering coefficient; (b) first derivative of the LIDAR signal; (c) Vertical profile of the backscattering coefficient measured at 12:00 (LST) with a dashed line showing the altitude of the cap of the mixing layer.

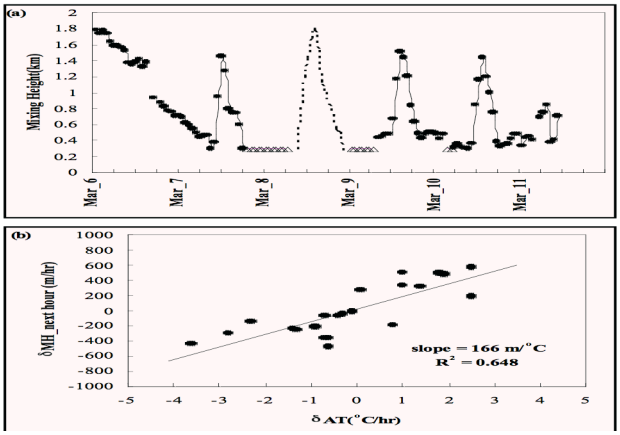


Fig. 3. (a) Hourly mixing height for the episode of this study. The open triangles denote that the mixing height was lower than the detectable range of our LIDAR system (0.3 km). (b) Linear correlation between the changes in ambient temperature and mixing height.

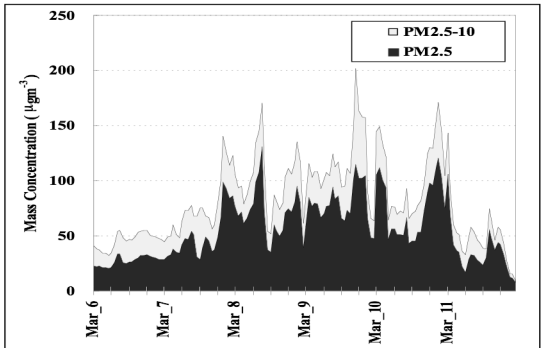


Fig. 4. Hourly variations of the concentrations of PM10 and PM2.5 during the episode of this study. The difference between PM2.5 and PM10 (shown in yellow) is the concentration of coarse particles (i.e. PM2.5-10).